Title

Oocyte Development and Quality in Young and Old Mice following Exposure to Atrazine

Journal

Environmental Health Perspectives, 130(11)

ISSN

0091-6765

Authors

Yun, Yan

Lee, Sunkyung

So, Christina

et al.

Publication Date

2022-11-01

DOI

10.1289/ehp11343

Peer reviewed

A Section 508–conformant HTML version of this article is available at https://doi.org/10.1289/EHP11343.

Oocyte Development and Quality in Young and Old Mice following Exposure to Atrazine

Yan Yun,[1,2] Sunkyung Lee,[1] Christina So,[1] Rushali Manhas,[1] Carol Kim,[1] Tabitha Wibowo,[1] Michael Hori,[1] and Neil Hunter[1,2,3]

[1]Department of Microbiology and Molecular Genetics, University of California, Davis, Davis, California, USA
[2]Howard Hughes Medical Institute, University of California, Davis, Davis, California, USA
[3]Department of Molecular and Cellular Biology, University of California, Davis, Davis, California, USA

Background: Egg development has unique features that render it vulnerable to environmental perturbation. The herbicide atrazine is an endocrine disruptor shown to have detrimental effects on reproduction across several vertebrate species.

Objectives: This study was designed to determine whether exposure to low levels of atrazine impairs meiosis in female mammals, using a mouse model; in particular, the study's researchers sought to determine whether and how the fidelity of oocyte chromosome segregation may be affected and whether aging-related aneuploidy is exacerbated.

Methods: Female C57BL/6J mice were exposed to two levels of atrazine in drinking water: The higher level equaled aqueous saturation, and the lower level corresponded to detected environmental contamination. To model developmental exposure, atrazine was ingested by pregnant females at 0.5 d post coitum and continued until pups were weaned at 21 d postpartum. For adult exposure, 2-month-old females ingested atrazine for 3 months. Following exposure, various indicators of oocyte development and quality were determined, including: *a*) chromosome synapsis and crossing over in fetal oocytes using immunofluorescence staining of prophase-I chromosome preparations; *b*) sizes of follicle pools in sectioned ovaries; *c*) efficiencies of *in vitro* fertilization and early embryogenesis; *d*) chromosome alignment and segregation in cultured oocytes; *e*) chromosomal errors in metaphase-I and -II (MI and MII) preparations; and *f*) sister-chromatid cohesion via immunofluorescence intensity of cohesin subunit REC8 on MI-chromosome preparations, and measurement of interkinetochore distances in MII preparations.

Results: Mice exposed to atrazine during development showed slightly higher levels of defects in chromosome synapsis, but sizes of initial follicle pools were indistinguishable from controls. However, although more eggs were ovulated, oocyte quality was lower. At the chromosome level, frequencies of spindle misalignment and numerical and structural abnormalities were greater at both meiotic divisions. *In vitro* fertilization was less efficient, and there were more apoptotic cells in blastocysts derived from eggs of atrazine-exposed females. Similar levels of chromosomal defects were seen in oocytes following both developmental and adult exposure regimens, suggesting quiescent primordial follicles may be a consequential target of atrazine. An important finding was that defects were observed long after exposure was terminated. Moreover, chromosomally abnormal eggs were very frequent in older mice, implying that atrazine exposure during development exacerbates effects of maternal aging on oocyte quality. Indeed, analogous to the effects of maternal age, weaker cohesion between sister chromatids was observed in oocytes from atrazine-exposed animals.

Conclusion: Low-level atrazine exposure caused persistent changes to the female mammalian germline in mice, with potential consequences for reproductive lifespan and congenital disease. https://doi.org/10.1289/EHP11343

Introduction

An egg that is competent for fertilization and development has a complex and protracted genesis that makes it uniquely vulnerable to environmental assaults.[1] Oogenesis begins during fetal development with germ-cell proliferation and differentiation into oogonia. Meiotic prophase I then ensues during which homologous chromosomes pair and undergo crossing over.[2] Crossovers, in combination with cohesion between sister chromatids, establish connections called chiasmata that direct accurate homolog disjunction during the meiosis-I division. In mammals, oocytes enter an extended arrest at the end of prophase I, coincident with the assembly of primordial follicles (in which the oocyte is surrounded by a single layer of flattened granulosa cells). Resumption of meiosis occurs only in follicles selected for maturation and ovulation.[3] Thus, female fecundity is shaped by the ability of arrested oocytes to maintain their integrity over a long life span (up to 50 y in humans). For these and other reasons, mammalian oocytes are innately prone to chromosome segregation errors,[4] with particularly high levels occurring in humans.[5] Moreover, segregation errors increase dramatically with advancing maternal age, due in large part to declining sister-chromatid cohesion.[5–10]

Oocyte number and quality can be impacted by a variety of intrinsic and extrinsic factors, including exposure to environmental contaminants. The herbicide atrazine (2-chloro-4-ethylamino-6-isopropylamino-*s*-triazine) is notable as a ubiquitous environmental contaminant and potent endocrine disruptor.[11] First registered as an herbicide in the1950s, atrazine is applied to agricultural and recreational lands worldwide.[12] The slow degradation of atrazine makes it a persistent contaminant of soil, surface water, and groundwater, and a frequent contaminant detected in drinking water.[13] The United States Environmental Protection Agency (U.S. EPA) has defined the safe limit in drinking water supplies as $\leq$3 μg/L,[14] whereas the World Health Organization (WHO) has set a much higher level of 100 μg/L.[15] Surface water contamination detected in agricultural areas is generally <2 μg/L, but levels >100 μg/L have been reported at some sites in the United States.[16,17] Atrazine exposure has been associated with neurotoxicity,[18] cancer,[18] and reproductive defects.[19] Acting as endocrine disruptors, environmental levels of atrazine caused defective steroidogenesis, gonadal dysgenesis, and hermaphroditism in amphibian[20] and fish models.[21]

In mammalian models, gestational atrazine exposure of male rats can alter hormone levels and delay puberty, although results

Address correspondence to Neil Hunter, Department of Microbiology and Molecular Genetics, University of California, Davis, 347C Briggs Hall, Davis, CA 95616 USA. Telephone: (530) 754-4401. Email: nhunter@ucdavis.edu

Supplemental Material is available online (https://doi.org/10.1289/EHP11343).

The authors declare they have no actual or potential competing financial interests.

Received 2 April 2022; Revised 10 October 2022; Accepted 17 October 2022; Published 11 November 2022.

have been somewhat conflicting. One study reported an increase in serum testosterone in male rat pups at 120 d postpartum (dpp),[22] whereas another study showed a decrease at 60 dpp.[23] Adult exposure in male rats was associated with reduced testosterone, delayed meiosis, and reductions in the number and quality of sperm.[24,25] Ominously, in mice, atrazine caused heritable epigenetic changes in the male germline.[26] An important finding is that an association between atrazine exposure and poor semen quality has been established in humans.[27] In female rodents, acute exposure to high levels of atrazine during gestation perturbed oocyte meiotic prophase I and the development of primordial follicles[28] and delayed puberty.[29] Exposure during adulthood was associated with increased levels of progesterone,[30] altered estrus cycles, and increased atretic follicles in rats.[31,32] However, the effects of atrazine exposure on oocyte meiotic divisions and the fidelity of chromosome segregation have not been analyzed.

An important caveat to many mammalian studies is the high exposure doses that are generally employed, levels that are unlikely to be encountered in the environment.[28,32,33] The exceptions detected increased progesterone, decreased oestradiol-17 beta, and altered estrus in sows that were exposed to just 2 mg/kg/d in feed for 19 d, raising concerns for human exposure and reproductive health.[34] Indeed, epidemiological studies suggest that atrazine exposure is associated with fetal growth retardation[35,36] and increased risk for preterm delivery,[37] though conflicting data exist.[38]

Whether environmentally relevant atrazine exposure impairs female reproduction and the specific processes that are impacted remain unclear. In this study, we chose female mice as an exposure model because methods to study meiotic chromosome metabolism in mouse oocytes are well established, and the fundamental processes are conserved in humans. By exposing mice to atrazine via drinking water we addressed: *a*) whether environmentally relevant levels of atrazine impact oocyte quality; *b*) the specific aspects of meiosis affected by atrazine, with a focus on chromosomal errors; *c*) whether exposure during development or adulthood have distinct effects; *d*) whether there are long-term effects on oocyte quality after exposure is terminated; and *e*) whether atrazine exposure during development compounds the effects of maternal age on oocyte quality.

Materials and Methods

Animals and Atrazine Exposure

Founder C57BL/6J mice (Stock No: 000664) were purchased from the Jackson Laboratory. Animals were maintained in a local vivarium with temperature control and a 12-h light/dark cycle. Weanling females (21 d postpartum; dpp) were housed, up to 4 per cage, with *ad libitum* access to standard rodent chow (Teklad global 18% protein; 2918, Envigo) and water. All animals were used for experimentation according to the guidelines of the Institutional Animal Care and Use Committees of the University of California, Davis (Protocol No. 21613). Atrazine (Molecular Formula: C8H14ClN5; Part No. N-11106-250MG; CAS: 1912-24-9; Purity: 99.3%) was purchased from Chem Service, Inc. For developmental exposure (Figure S1A), 33 mg/L (high dose) or 100 μg/L (low dose) atrazine-containing drinking water was supplied to 2-month-old pregnant females at embryonic day 0.5 (E0.5) until either euthanasia at embryonic day 18.5 (E18.5) or until pups were weaned at 21 dpp. Weanling females were euthanized for oocyte analysis at 3 months old unless noted otherwise. For adult ovary exposure (Figure S1E), 2-month-old females were supplied with high- or low-dose atrazine-containing drinking water for 3 months prior to euthanasia and oocyte analysis. E18.5 fetuses were euthanized by surgical decapitation, and other mice were euthanized by carbon dioxide asphyxiation. 33 mg/L was selected as the high dose because atrazine reaches saturation at this concentration in water at 25°C[39] and is therefore the maximum level that could be encountered in contaminated water. Given an average water intake of 5 mL per day and average body weight of 20 g for an adult female, 33 mg/L is equivalent to a dose of ∼8.25 mg/kg/d. 100 μg/L (a dose of ∼25 μg/kg/d) was selected as the low dose because this is the level set as the safe limit in drinking water by the WHO[15] and has been detected in contaminated water at some sites in the United States.[16,17] Littermates or age-matched females were allocated to treatment groups randomly. Body weight was measured at 3-months old or 5-months old, following exposure during development (Figure S1A) or adulthood (Figure S1E), respectively. Gestation time was the period from timed mating to the observation of newly born pups during daily litter checks; litter size was counted at the same time. Pup mortality was determined by comparing the numbers of pups observed at birth and at weaning (21 d postpartum). The two atrazine doses employed here did not impact body weight, gestation time, litter size, or pup mortality (Figure S1), indicating that our exposure regimens do not cause gross toxic effects.

Oocyte Collection and In Vitro *Maturation*

Germinal vesicle (GV)–stage oocytes were released from the dissected ovaries of experimental animals without prior hormonal stimulation, by multiple punctures with a 25G needle (BD PrecisionGlide) under a stereo microscope (SMZ1500, Nikon). Only oocytes with integral cumulus cell layers were used. Oocytes were collected and cultured in M2 medium (M7167, Sigma-Aldrich) under mineral oil (M8410, Sigma-Aldrich and NO-100, Nidacon) at 37°C for *in vitro* maturation after mechanically removing surrounding cumulus cells for observation of germinal-vesicle breakdown (GVBD) and polar body extrusion (PBE). GVBD was scored after 3 h of culture. Only oocytes that underwent GVBD within 3 h were used to quantify PBE after a further 13 h of incubation.

Chromosome Preparations from Metaphase Oocytes and Immunofluorescence

MI and MII oocytes were acquired after 7 h and 16 h of culture in M2 medium at 37°C, respectively. Metaphase chromosomes were prepared as previously described.[40] Briefly, Acid Tyrode's solution (M1788, Sigma-Aldrich) was applied to remove zona pellucida, and zona-free oocytes were spread on glass slides in 1% paraformaldehyde (19208; Electron Microscopy Science) with 0.15% Triton X-100 (X100; Sigma-Aldrich) and 3 mM DTT (D8070, USBiological) in H_2O pH9.2. To improve the accuracy of chromosome counting, a single oocyte was prepared in each well of a 12-well slide (63425-05, Electron Microscopy Science). Chromosome preparations were air-dried at room temperature overnight.

All of the following procedures were performed at room temperature. MI and MII oocyte chromosome preparations were incubated in blocking solution (10% normal goat serum, 3% BSA, 0.05% Triton X-100, 0.05% Sodium azide in TBS) for 1–2 h, followed by an overnight incubation with primary antibodies: human anticentromere antibody (ACA or CREST; 1:1,000 dilution; HCT-0100, ImmunoVision) and rabbit anti-REC8 antibody (1:100 dilution; a kind gift from Dr. Scott Keeney, Memorial Sloan-Kettering Cancer Center). After three washes in blocking solution, slides were incubated for 1 h with goat antihuman 555 (1:1,000 dilution; A-21433, Thermo Fisher Scientific), and goat anti-rabbit 488 (1:1,000; A-11034, Thermo Fisher Scientific)

secondary antibodies. Chromosomes were stained with 4′,6-diamidino-2-phenylindole at a concentration of 5 μg/mL (DAPI; D8417; Sigma-Aldrich).

Surface-Spread Preparations of Fetal Oocyte Nuclei and Immunofluorescence

Fetal ovaries were dissected from E18.5 female fetuses and processed for surface spreading of prophase-I oocyte nuclei as described.[40] Briefly, ovaries were incubated in hypotonic extraction buffer (50 mM sucrose, 30 mM Tris–HCl pH 8.0, 17 mM trisodium citrate, 5 mM EDTA, 0.5 mM DDT, and 0.5 mM PMSF) on ice for 20 mins and then minced in a 20-μL drop of 0.1 M sucrose (S0389, Sigma-Aldrich). The cell suspension was spread on a slide (12-544-7, Fisher Scientific) coated in 1% paraformaldehyde with 0.15% Triton X-100 in H_2O pH 9.2 and air-dried overnight in a humid chamber. Finally, the slides were washed in 0.4% Photo Flo (1464510, Kodak) and dried again at room temperature.

Immunofluorescence staining was performed using the following primary antibodies with incubation overnight at room temperature after blocking at room temperature for 1 h: rabbit anti-SYCP3 (1:200; sc-33195, Santa Cruz), mouse anti-MLH1 (1:25; 3515, Cell Signaling Technology), human anticentromere antibodies (ACA or CREST; 1:1,000; HCT-0100, ImmunoVision). Slides were subsequently incubated with the following goat secondary antibodies for 1 h at room temperature: anti-rabbit 568 (1:1,000; A11036, Thermo Fisher Scientific), antimouse 488 (1:1,000; A11029, Thermo Fisher Scientific), and antihuman DyLight 649 (1:200; 109-495-088, Jackson Labs). Coverslips were mounted with ProLong Diamond antifade reagent (P36970, Thermo Fisher Scientific) prior to imaging.

Spindle Staining of Metaphase I and II Oocytes

For analysis of chromosome alignment, MI and MII oocytes were acquired after 9 h and 16 h of culture in M2 medium at 37°C, respectively. Intact oocytes were fixed and permeabilized in 2% paraformaldehyde in PHEM buffer (60 mM PIPES, 25 mM HEPES, 25 mM EGTA, 4 mM MgSO4) with 0.5% Triton X-100. Blocking was performed in 7% normal goat serum (10000C, Thermo Fisher Scientific) in phosphate-buffered saline (PBS) with 0.1% Tween-20 for overnight. Primary mouse anti-α tubulin monoclonal antibody (A11126, Thermo Fisher Scientific; diluted 1:400 in PBS with 3% BSA, 0.1% Tween-20) was then added and incubated overnight at 4°C. Secondary antibody was goat antimouse 488 (1:1,000; A11029, Thermo Fisher Scientific), incubated for 1 h at room temperature. Chromosomes were stained with Hoechst (H3569, Thermo Fisher Scientific; 20 μg/mL) prior to mounting in ProLong Diamond antifade reagent.

In Vitro *Fertilization and Terminal Deoxynucleotidyl Transferase dUTP Nick End Labeling (TUNEL) Assay on Blastocysts*

Adult females were hormonally primed with intraperitoneal injection of 5.0 IU pregnant mares' serum gonadotrophin (G4877-2000IU, Sigma-Aldrich), followed by injection of 5.0 IU human chorionic gonadotropin (hCG; CG10, Sigma-Aldrich) 48 h later. At 13–14 h after hCG injection, female mice were euthanized by carbon dioxide asphyxiation, and metaphase II eggs were retrieved from oviducts by tearing the ampulla with a 25G needle (BD PrecisionGlide) under a stereo microscope (SMZ1500, Nikon). Eggs were transferred to human tubal fluid (MR-070-D, Millipore Sigma) and immediately incubated with freshly prepared sperm at a final concentration of $1–2 \times 10^6$ per mL. Sperm were freshly isolated from cauda epididymides of a control (unexposed) male (2 to 5 months old) euthanized by carbon dioxide asphyxiation. Specifically, cauda epididymides were cut with scissors, and sperm were squeezed out using pressure from a 25G needle (BD PrecisionGlide) under a stereo microscope (SMZ1500, Nikon). Sperm were incubated in CARD FERTIUP Preincubation Medium (KYD-002-EX, Cosmo Bio) for 60 mins prior to use for *in vitro* fertilization. After 4 h of sperm–egg incubation, sperm and cumulus cells were mechanically removed from the eggs/zygotes by repeated pipetting and then transferred to KSOM medium (MR-106-D, Millipore Sigma) for further culture. After 24 h, 2-cell stage embryos were scored as a readout of fertilization efficiency; 4-cell and blastocyst stage embryos were subsequently scored at 48 and 108 h, respectively.

Blastocysts were fixed and permeabilized in 4% paraformaldehyde in PBS with 0.5% Triton X-100. After washing in PBS, blastocysts were subject to the TUNEL reaction using the In-Situ Cell Death Detection Kit (11684809910, Roche) according to the manufacturer's instructions. Hoechst (20 μg/mL) was added to fluorescently stain nuclei.

Image Acquisition and Analysis

For prophase-I and metaphase oocyte chromosomes preparations, images were acquired using a Zeiss AxioPlan II microscope equipped with a 63× oil immersion objective and Hamamatsu ORCA-ER CCD camera. Image processing and analysis were performed using Volocity (version 6.3; Perkin Elmer) and ImageJ [version 1.53o; National Institutes of Health (NIH)] software.

For immunostaining of intact metaphase oocytes and blastocysts, three-dimensional imaging was performed using a Zeiss Airyscan LSM 800 confocal equipped with a 63× oil immersion objective and Axiocam camera. Spindles and chromosomes in metaphase oocytes were imaged with a *z*-resolution of 2.0 μm, and blastocysts were captured every 5.0 μm until the entire oocyte or embryo was covered. ImageJ (version 1.53o; NIH) software was used for image processing and analysis.

To quantify fluorescence intensities of REC8 immunostaining, metaphase-I chromosomes from the three experimental groups were prepared and processed in parallel, and images were acquired on the same day using identical exposure settings. Individual chromosomes were selected manually using DAPI staining, and the associated mean gray values were measured for REC8 and CREST channels, subtracting background signals. Relative chromosomal REC8 intensities were calculated as a ratio of REC8 to CREST, and an average for all chromosomes in each individual metaphase-I oocyte was calculated to generate the data points shown in Figure 5F. Three independent experiments were pooled by normalizing to the mean values for oocytes from each control. For interkinetochore distances (IKDs) in metaphase-II chromosomes (Figure 5B), distances between the centers of the two CREST foci within a pair of sister chromatids were measured, and then the average from all measurements in an individual metaphase-II egg was calculated to generate the data points shown in Figure 5C.

Confocal Time-Lapse Imaging

GV-stage oocytes were cultured *in vitro* for 2 h, when the majority had completed GVBD. Oocytes with GVBD were then incubated with 100 nM SiR-DNA (CY-SC007, Cytoskeleton) in M2 medium to label chromosomes. Next, 4-dimensional imaging was performed using a Zeiss Airyscan LSM 800 confocal equipped with a 40x water immersion objective and Axiocam camera, or a 3i Spinning Disk confocal equipped with a 63x oil immersion objective lens and Flash 4.0 sCMOS camera. Both were equipped with a 37°C temperature-controlled environment. Chromosomes

were imaged with 18 z-sections and 2.0 µm z-resolution. The imaging time between consecutive frames was 6 min. To capture the events of chromosome alignment and segregation, imaging was performed between 9 and 12 h of culture. SiR-DNA containing M2 medium was used throughout the imaging procedure.

Statistical Analyses

For all comparisons, a minimum of two independent experiments were performed. For each developmental exposure group (unexposed control, low-dose, and high-dose atrazine), 3–16 females from 2–7 different litters were examined, unless otherwise stated. The numbers of mice and litters used for each experiment are stated in the figure legends.

An intrinsic limitation to statistical analysis of oocyte phenotypes is the small numbers of analyzable eggs that can be obtained from individual females. Therefore, oocyte samples from independent experiments are typically pooled to calculate proportions, and comparisons are made via Fisher's exact tests.[41,42] Error bars for analysis of such data indicate the standard error of a proportion.[5] All other mean analyses were performed using either Student's t or Mann-Whitney tests for two group comparisons, Ordinary one-way analysis (ANOVA) and post hoc Dunnett's tests were used for three group comparisons and presented as mean ± standard deviation (SD). Data were processed using GraphPad Prism 8 (version 9.4.1; Dotmatics), with a significance threshold of $p < 0.05$. All statistical tests and significance levels are reported in the figure legends. The summary cartoon in Figure 7 was created with Microsoft PowerPoint (version 16.27; Microsoft).

Results

Atrazine Exposure during Development: Meiotic Prophase-I, Fertilization, and Early Embryogenesis

The early events of female meiosis and oogenesis are susceptible to perturbations that can reduce the size and quality of ovarian reserves and thereby impact lifetime reproductive success. Key events of meiotic prophase I, including homolog pairing, synapsis, and crossing over, occur *in utero*; then around birth, meiosis arrests, and oocytes assemble into primordial follicles to establish initial ovarian reserves.[43] To determine the effects of atrazine on these critical early events, animals were exposed throughout gestation and early postnatal development by supplying dams with contaminated drinking water while pregnant and nursing, until pups were weaned (Figure 1A). This "developmental" exposure regimen was terminated at E18.5 for the analysis of prophase-I events in fetal ovaries, at 18 dpp for the quantification of ovarian reserves, or at weaning (21 dpp) for subsequent analysis of oocyte quality.

Prophase-I nuclei with one or more defects of chromosome synapsis, including asynapsis and nonhomologous pairing of chromosome axes (Figure 1B), were ∼3-fold higher in oocytes from atrazine-exposed fetuses [from 5.4% of cells in unexposed controls, to 16.5% and 15.2% in low (100 µg/L, ∼25 µg/kg/d) and high (33 mg/L, ∼8.25 mg/kg/d) exposure groups, respectively; $p < 0.01$; Figure 1C; see Excel Table S1]. Despite higher levels of synaptic irregularities, crossover numbers, quantified using the crossover specific marker MLH1, were not significantly different (Figure 1D,E). Comparison of the distributions of MLH1 foci suggests slightly more (6.9%) chromosomes with a single crossover at the expense of chromosomes with ≥2 crossovers (7.9% lower), but only at the higher atrazine dose (Figure 1F; $p = 0.0125$, in comparison with unexposed controls; see Excel Tables S2 and S3 for raw and summary data, respectively). However, the frequency of chromosomes lacking an MLH1 focus, indicative of crossover failure, was not different.

Prophase-I defects, such as asynapsis, can lead to oocyte apoptosis and thus lower numbers of primordial follicles.[43] However, ovarian reserves (follicle number per ovary from 18 dpp mice) were indistinguishable from unexposed controls (Figure 1G), indicating that oocyte survival was not significantly impacted by the elevated synaptic errors seen in oocytes from atrazine-exposed females (Figure 1B,C). Atrazine exposure was associated with a slightly higher levels of follicles containing more than one oocyte, suggesting that the breakdown of germline cysts (the clusters of oocytes that precede follicle formation)[44] is perturbed by atrazine exposure (Figure 1H,I).

The quality of oocytes following developmental atrazine exposure was assessed by measuring the efficiency of *in vitro* fertilization (IVF) and early embryogenesis (2 and 4-cell embryos and blastocyst formation; Figure 2). Metaphase-II (MII) arrested eggs were obtained for IVF from super-ovulated females age 3–6 months, i.e., 10–23 wk after atrazine exposure was terminated at weaning. Surprisingly, the number of eggs retrieved from animals exposed to a high dose of atrazine was 1.7-fold higher relative to unexposed controls (Figure 2A, $p = 0.0346$, one-way ANOVA and Dunnett's tests). This observation points to hyperstimulation of follicle growth and resumption of meiosis or perhaps to reduced apoptosis (atresia) of growing follicles. However, both low- and high-dose atrazine exposure was associated with higher levels of dead or dying MII eggs with fragmented cellular contents. Only 2.6% of eggs (4/155) from unexposed females were fragmented in comparison with 8.5% (15/176) and 9.0% (23/256) from low- and high-dose exposure cohorts, respectively ($p = 0.0307$ and $p = 0.0125$, respectively; Fisher's exact test; Figure 2B).

To determine the developmental capacity of oocytes, intact MII eggs from exposed and control animals were fertilized with sperm from unexposed males. 60.2% of eggs (65/108) from unexposed females formed 2-cell embryos 24 h after eggs and sperm were mixed (Figure 2C). IVF efficiency was around one-third lower for eggs from atrazine-exposed animals, down to 40.8% (51/125) and 43.7% (86/197) 2-cell embryos from the low- and high-dose groups, respectively ($p = 0.0038$ and $p = 0.0061$, respectively; Fisher's exact test). In embryos that successfully traversed the 2-cell stage, the efficiency of 4-cell embryo and blastocyst formation was indistinguishable between exposed and unexposed groups (Figure 2C). Blastocyst integrity was assessed by counting total cell number, and the percentage of cells that were apoptotic (Figure 2D–F). Total cell number did not differ for blastocysts derived from atrazine-exposed and control groups (Figure 2E). However, both low- and high-dose atrazine exposure were associated with ∼2-fold higher levels of TUNEL-positive apoptotic cells ($10.4 \pm 4.6\%$ and $10.0 \pm 5.9\%$ in low- and high-dose exposures vs. $4.0 \pm 3.1\%$ in unexposed controls, mean ± S.D; $p = 0.0054$ and $p = 0.0037$, respectively, one-way ANOVA and Dunnett's tests; Figure 2F; see Excel Table S10). Moreover, in blastocysts derived from eggs of atrazine-exposed animals, the fraction of cells that were apoptotic was very variable, ranging from 1.7% to 22.2%.

Chromosome Misalignment and Missegregation in Oocytes from Atrazine-Exposed Animals

To better understand the etiology of lower egg quality following atrazine exposure during development, we cultured GV-stage oocytes and analyzed chromosome integrity and segregation at meiosis I. Atrazine exposure did not perturb maturation, with very similar efficiencies of meiotic resumption and completion of meiosis I observed for oocytes from all three exposure groups (assayed respectively via GVBD and first PBE; Figure S2A–C).

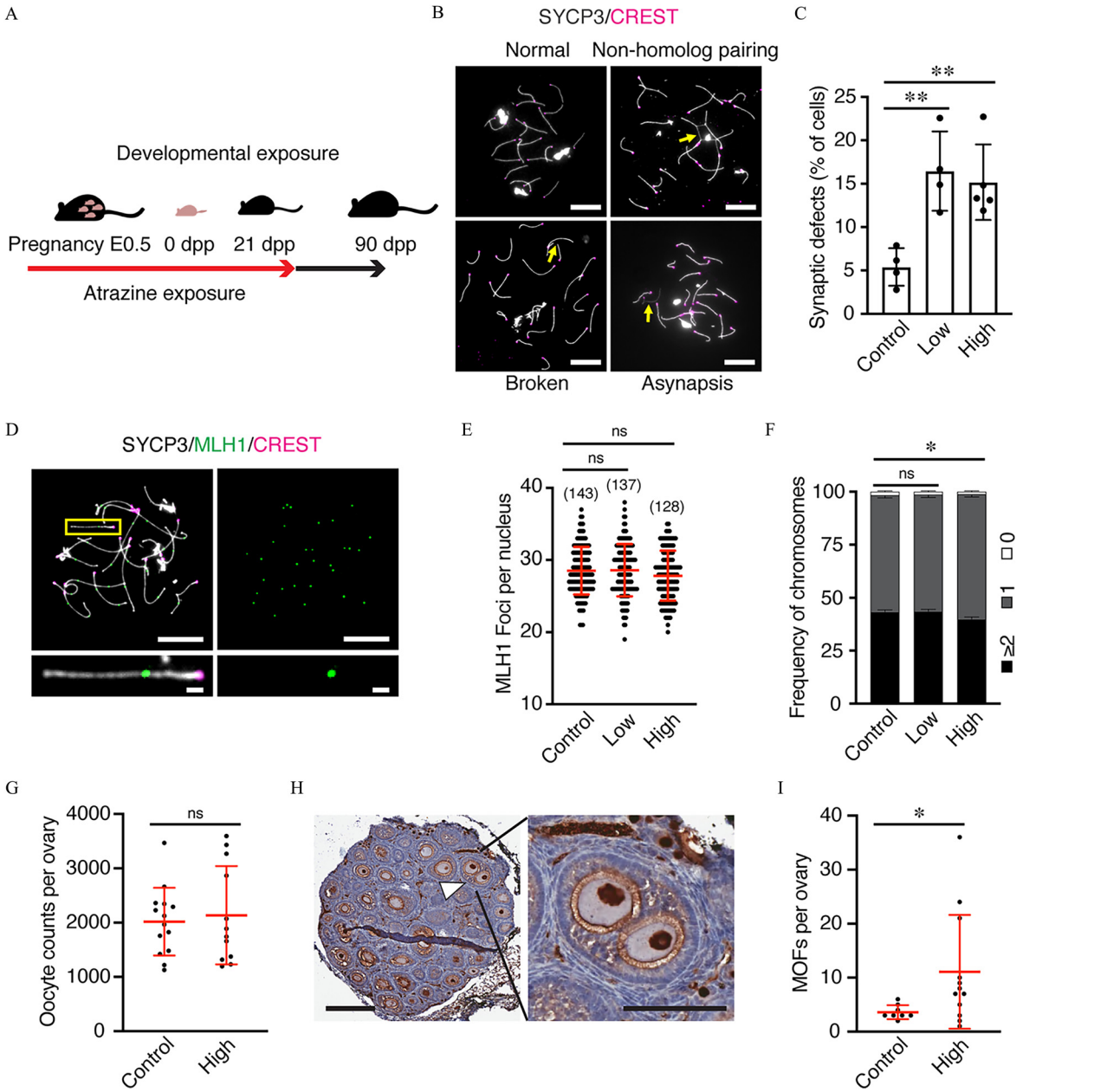

Figure 1. Analysis of meiotic prophase I, ovarian reserves, and MOFs following atrazine exposure during development. (A) Schematic of developmental atrazine exposure regimen. (B) Representative images of prophase-I oocyte chromosome preparations from E18.5 embryos immunostained for SYCP3 (gray), to label homolog axes, and CREST (magenta), to label centromeres. Examples of pachytene-stage nuclei with normal synapsis, nonhomologous pairing, broken axes, and asynapsis are shown. Yellow arrows indicate synaptic defects. Scale bars represent 10 μm. (C) Quantification of synaptic defects across litters (numbers of animals and litters used to generate data: control, 6 animals and 4 litters; low dose, 6 and 4; high dose 9 and 5; also see Excel Table S1). (D) Representative pachytene-stage oocyte chromosomes immunostained for SYCP3 (gray), CREST (magenta) and the crossover marker MLH1 (green). A single synapsed chromosome pair is magnified in the bottom panels. Scale bars represent 10 μm (main panels) and 1 μm (magnified panels). (E) Quantification of MLH1 foci per nucleus (also see Excel Table S2). (F) Distributions of MLH1 focus numbers per chromosome (also see Excel Table S3). Percentages of chromosomes with 0, 1, and ≥2 MLH1 foci are plotted for the three exposure groups [2,860, 2,740, and 2,560 chromosomes in control, low, and high groups, respectively; numbers of animals and litters used to generate the data in (E) and (F): control, 10 and 4; low, 8 and 4; high 6 and 3]. (G) Total oocyte counts per ovary from 18 dpp females (numbers of animals and litters used to generate the data: control, 7 and 6; high 6 and 2. Both ovaries from individual animals were analyzed; also see Excel Table S4). (H) Representative ovary section from an 18 dpp female exposed to a high dose of atrazine, immunostained for p63 to mark oocyte nuclei and counterstained with hematoxylin. The white caret indicates an MOF containing two oocytes that is magnified in the right panel. Scale bars represent 200 μm (left panel) and 100 μm (right panel). (I) Numbers of MOFs per ovary (numbers of animals and litters used to generate the data: control, 4 and 2; high 6 and 2. Both ovaries from individual animals were analyzed; also see Excel Table S5). Bidirectional error bars in (C), (E), (G), and (I) represent mean ± standard deviation; unidirectional error bars in (F) represent standard error of a proportion. Data were analyzed with ordinary one-way ANOVA Dunnett's multiple comparisons tests (C) and (E), unpaired *t* test (G) and Mann-Whitney test (I). The chi-square test was applied in (F) to compare distributions of MLH1 focus numbers. Low, 100 μg/L; High, 33 mg/L. Note: ANOVA, analysis of variance; dpp, days postpartum; E0.5, embryonic day 0.5; MOF, multi-oocyte follicle; ns, not significant. $^{*}p < 0.05$; $^{**}p < 0.01$.

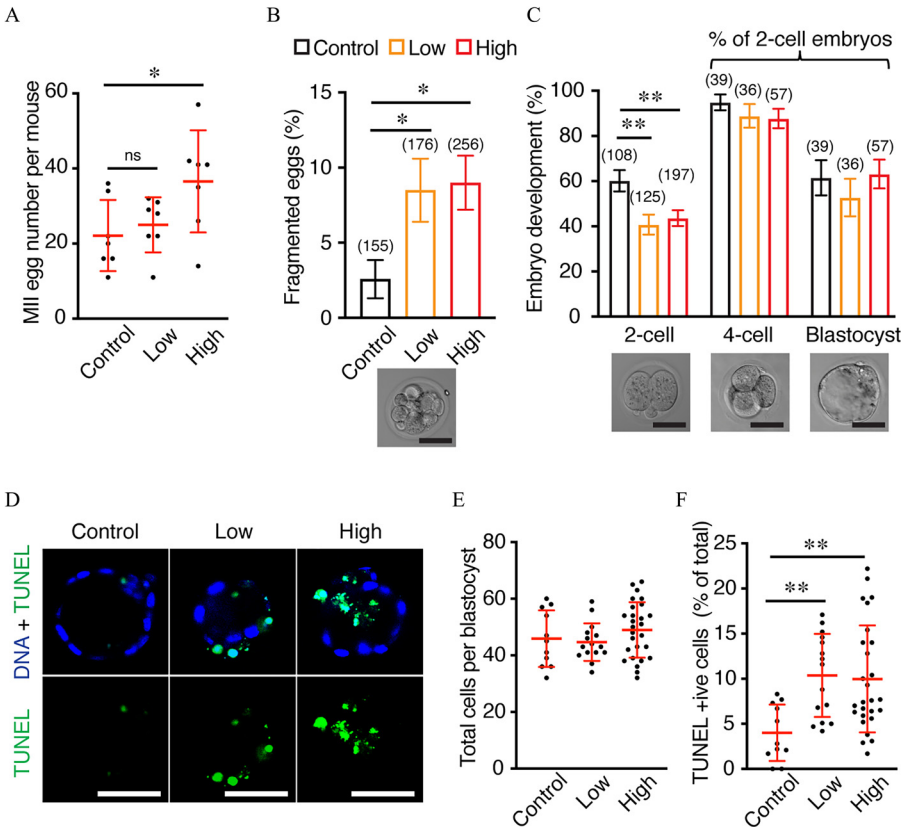

Figure 2. *In vitro* fertilization and preimplantation embryo development following atrazine exposure during development. (A) Numbers of MII eggs collected from superovulated females (also see Excel Table S6). (B) Fractions of MII eggs that were fragmented [numbers of fragmented and unfragmented eggs provided in Excel Table S7; representative image is shown below; numbers of animals and litters used to generate data in (A) and (B): control, 7 animals and 4 litters; low dose, 7 and 3; high dose, 7 and 3]. (C) Efficiencies of *in vitro* fertilization (2-cell embryos) and preimplantation embryo development (actual numbers of embryos in each stage of development are provided in Excel Table S8. Representative images are shown below. Efficiencies of 4-cell embryo and blastocyst formation are expressed as percentages of 2-cell embryos; number of animals and litters to generate data for 2-cell embryos are 5 and 3, 6 and 3, 5 and 2 in each exposure group; number of animals and litters to generate data for 4-cell embryos and blastocysts are 3 and 2 in each exposure group). (D) Representative images of single *z*-sections of blastocysts derived from *in vitro* fertilization, stained for DNA (Hoechst; blue) and TUNEL (green). (E) Total cell numbers per blastocyst (also see Excel Table S9). (F) Percentage of blastocyst cells that were TUNEL positive. Numbers of animals and litters used to generate data in (E) and (F) were 3 and 2, 2 and 2, and 3 and 2 in control, low, and high exposure groups, respectively; also see Excel Table S10. Numbers of eggs (B) or embryos (C) analyzed are indicated in parentheses above the bars. Bidirectional error bars represent mean ± standard deviation (A,E,F) or standard error of a proportion (B,C). Data in A, E, and F were analyzed with one-way ANOVA and Dunnett's tests; B and C were analyzed with Fisher's exact tests. Scale bars in B–D represent 50 μm. Low, 100 μg/L atrazine; High, 33 mg/L. Note: ANOVA, analysis of variance; MII, metaphase II; ns, not significant; TUNEL, terminal deoxynucleotidyl transferase dUTP nick end labeling. $^{*}p < 0.05$; $^{**}p < 0.01$.

Metaphase-I abnormalities. Chromosome congression is particularly important for accurate segregation in mammalian oocytes because the spindle assembly checkpoint is less robust in meiosis, such that misaligned chromosomes can escape and missegregate.[4,45] Congression at metaphase I (MI) was analyzed in fixed oocytes fluorescently stained to visualize spindles and chromosomes (Figure 3A). Defects were classified as mild, with 1 or 2 misaligned chromosomes, or severe with ≥3 misaligned chromosomes (Figure 3A); 16.3% (7/43) of control oocytes showed chromosome misalignment; 14.0% (6/43) were classified as mild, and only 2.3% (1/43) were classified as severe (Figure 3B). In low- and high-dose atrazine groups, misalignment was seen in 33.3% (10/30) and 36.5% (19/52) of oocytes, respectively, with 16.7% (5/30) and 25.0% (13/52) showing severe misalignment. Statistical analysis of the distributions of the three alignment classes showed significantly more chromosome misalignment for the high-dose group ($p = 0.0050$, Fisher's exact test) but not for the low-dose group ($p = 0.0950$). Misalignment in MI predicts chromosome missegregation at anaphase I. To test this inference, live-cell imaging was used to quantify meiosis I chromosome missegregation, i.e., NDJ and lagging chromosomes (Figure 3C; Movies S1–S3). Missegregation was detected in 12.7% of control oocytes (7/55; Figure 3D), a higher frequency than those reported in the literature (≤5%[6,46]), which appeared to be caused by the SiR-DNA fluorogenic DNA label (Spirochrome) used to visualize chromosomes. Notwithstanding this higher baseline, oocytes from animals exposed to the higher dose of atrazine had more than twice as many chromosome segregation errors as unexposed controls [(26.9%, 28/104), $p = 0.0453$, Fisher's exact test]. Thus, consonant with our analysis of fixed cells, atrazine exposure during development was associated with higher levels of chromosome misalignment and missegregation at meiosis I.

Metaphase-II abnormalities. Chromosome misalignment and missegregation during meiosis I are expected to manifest as chromosomal abnormalities in the succeeding MII–arrested eggs. To test this prediction, oocytes from control animals and animals exposed to atrazine during development were cultured through to MII arrest and chromosomes prepared for immunofluorescence imaging. Euploid MII mouse eggs contain 20 pairs of sister chromatids connected at their centromeric ends, whereas aneuploid eggs have either extra or missing sister chromatid pairs. A second type of chromosomal abnormality—predivision or precocious separation of sister chromatids—results in free single chromatids that are expected to segregate

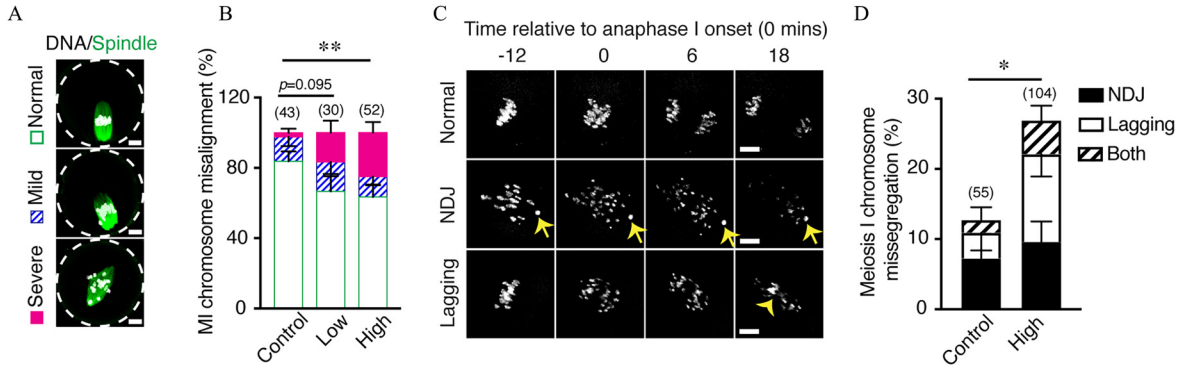

Figure 3. Chromosome alignment and segregation in meiosis-I oocytes following atrazine exposure during development. (A) Representative images of MI oocytes, stained for spindles (α-tubulin, green) and DNA (Hoechst, white), illustrating classes of chromosome misalignment. (B) Quantification of chromosome misalignment in the MI oocytes represented in panel A (data generated from 5 animals from 3 litters in each exposure group; see Excel Table S11). (C) Live-cell images from selected timepoints of meiosis-I stage oocytes showing examples of normal chromosome segregation, NDJ, and lagging segregation. Arrows highlight a NDJ event. The arrowhead highlights lagging chromosomes. (D) Quantification of chromosome missegregation in meiosis-I oocytes. Data generated from 7 animals and 5 litters (unexposed control); and 8 animals and 4 litters (high-dose atrazine), respectively (also see Excel Table S12 for summary data). Numbers of oocytes examined in (B) and (D) are indicated in parentheses above the bars. Error bars represent standard error of a proportion; unidirectional bars are shown for the individual classes to avoid overlaps. Data in (B) and (D) were analyzed with Fisher's exact tests. Statistical analysis performed in (B) compares the distributions of the three alignment classes shown in (A). All missegregation types were combined for the statistical analysis in (D). Scale bars in (A) and (C) represent 10 μm. Low, 100 μg/L atrazine; High, 33 mg/L. Note: MI, metaphase I; NDJ, nondisjunction. $^{*}p < 0.05$; $^{**}p < 0.01$.

randomly during meiosis II (following fertilization) and are therefore a high risk for embryo aneuploidy (Figure 4A). Consistent with previous studies in the C57BL/6J mouse strain,[47] only 1.0% of control eggs (1/105) were chromosomally abnormal. By comparison, chromosomal abnormalities were seen in 7.4% (4/54) and 14.9% (7/47) of eggs from the low- and high-dose atrazine exposure groups, respectively ($p = 0.0458$ and $p = 0.0012$, respectively, Fisher's exact test; Figure 4B).

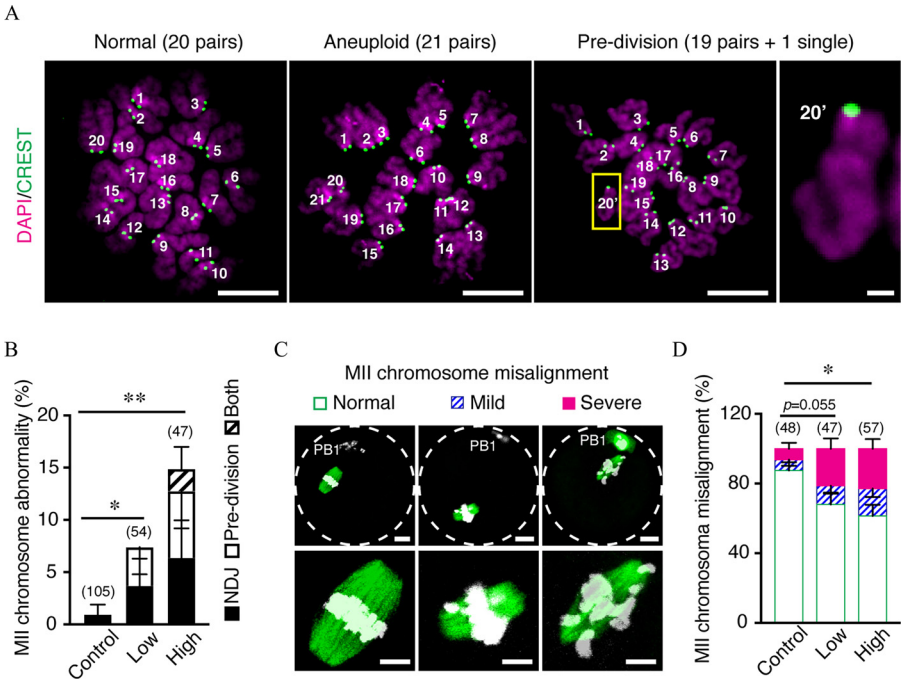

Figure 4. Analysis of chromosomal abnormalities and alignment in metaphase-II eggs following atrazine exposure during development. (A) Representative images of MII oocyte chromosomes showing normal euploid (20 pairs of sister chromatids) and aneuploid (21 pairs) nuclei, and a cell with a single free chromatid (20'; magnified in the right-hand side panels) indicative of a premature separation event (predivision). Centromeres (green) were immunostained with CREST, and chromosomes (magenta) were counterstained with DAPI. Scale bars represent 10 μm (main panels) and 1 μm (magnified panel). (B) Quantification of chromosomal abnormalities in MII eggs from 3-month-old mice. Numbers of animals used were 8 (from 7 litters; unexposed control), 4 (from 3 litters; low dose) and 5 (from 3 litters; high dose), respectively (also see Excel Table S13 for the summary data). (C) Representative images of MII eggs, stained for spindles (α-tubulin, green) and DNA (Hoechst, white), illustrating classes of chromosome misalignment. PB1, indicates the position of the first polar body. Scale bars represent 10 μm (top panels) and 5 μm (lower panels). (D) Quantification of chromosome misalignment in the metaphase-II eggs represented in (C). 3 animals were used for each exposure group, from 3 (control), 3 (low), and 2 (high) litters, respectively (also see Excel Table S14 for summary data). Numbers of eggs examined in (B) and (D) are indicated in parentheses above the bars. Error bars represent standard error of a proportion; unidirectional bars are shown for the individual classes to avoid overlaps. Data in (B) and (D) were analyzed with Fisher's exact tests. All missegregation types were combined for the statistical analysis in (B). Statistical analysis performed in (D) compares the distributions of the three alignment classes shown in (C). Low, 100 μg/L atrazine; High, 33 mg/L. Note: MII, metaphase II; NDJ, nondisjunction. $^{*}p < 0.05$; $^{**}p < 0.01$.

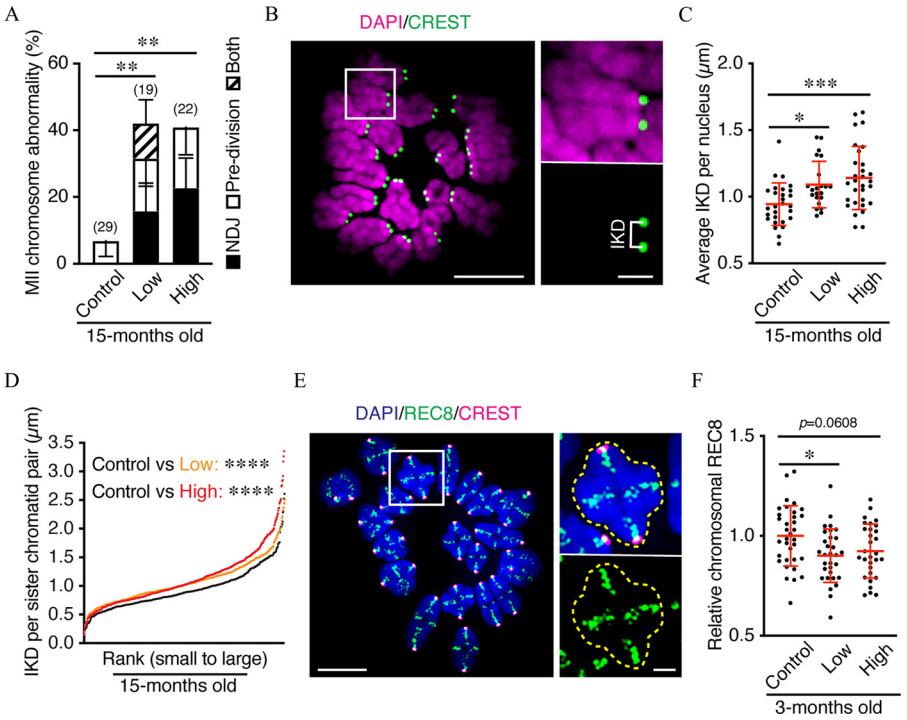

Figure 5. Analysis of chromosomal abnormalities and sister-chromatid cohesion in oocytes of aged mice following atrazine exposure during development. (A) Quantification of chromosomal abnormalities in MII eggs from 15-month-old mice. Numbers of animals used were 8 (from 4 litters; unexposed control), 6 (from 2 litters; low dose), and 5 (from 2 litters; high dose), respectively (also see Excel Table S15 for summary data). (B) Representative image of MII chromosomes illustrating the measurement of IKD for a single chromatid pair (magnified panels). Kinetochores (green) were immunostained with CREST, and chromosomes (magenta) were counterstained with DAPI. Scale bars represent 10 μm (main panel) and 2 μm (magnified panels). (C) Average IKDs per nucleus for MII eggs from 15-month-old mice (also see Excel Table S16). (D) Rank distributions of IKDs for individual sister-chromatid pairs of MII eggs from 15-month-old mice. Numbers of sister-chromatid pairs examined in each group were 546 (28 cells, unexposed control), 422 (22 cells, low dose), and 575 (30 cells, high dose), respectively. Numbers of animals used in (C) and (D) were 8 (from 4 litters), 6 (from 2 litters), and 5 (from 2 litters) in control, low-, and high-dose groups, respectively; also see Excel Table S17. (E) Representative image of MI oocyte chromosomes, immunostained for meiosis-specific cohesin component REC8 (green), centromere marker CREST (magenta) and counterstained with DAPI (blue). The right-hand side panels show a single homolog pair; the dashed line highlights the area in which fluorescent intensity was measured to quantify chromosome-associated REC8 (details in the "Materials and Methods" section). Scale bars represent 10 μm (main panel) and 2 μm (magnified panel). (F) Quantification of average chromosomal REC8 level per MI oocyte nucleus from 3-month-old mice. Numbers of animals used were 4 (from 3 litters; unexposed control), 4 (from 3 litters; low dose), and 5 (from 3 litters; high dose), respectively; also see Excel Table S18. Numbers of eggs examined in (A) are indicated in parentheses above the bars; error bars in (A) show standard error of a proportion; unidirectional bars are shown to avoid overlaps. Bidirectional error bars in (C) and (F) indicate mean ± standard deviation. Data were analyzed with Fisher's exact tests (A), and one-way ANOVA and Dunnett's tests (C,D,F), respectively. MII chromosomal abnormalities were combined for statistical analysis in (A). Low, 100 μg/L atrazine; High, 33 mg/L. Note: ANOVA, analysis of variance; IKD, interkinetochore distance; MI, metaphase I; MII, metaphase II; NDJ, nondisjunction. $^{*}p < 0.05$; $^{**}p < 0.01$; $^{***}p < 0.001$; $^{****}p < 0.0001$.

Chromosome alignment in MII oocytes was also examined. As predicted from the high levels of chromosome abnormalities seen in oocytes from atrazine-exposed animals, ≥30% (15/47 and 22/57) of MII oocytes from the low- and high-dose groups showed misalignment, with severe defects (≥3 chromosomes) being seen in >20% (10/47 and 13/57) of cells (Figure 4C,D). Again, comparison of the distributions showed that this effect was only significant in the high-dose group ($p = 0.0551$ and $p = 0.0101$ for the low- and high-dose groups, respectively); however, when analyzed as a simple proportion, there were significantly higher levels of cells with chromosome misalignment (mild + severe) in the low-dose group ($p = 0.0270$). Misalignment in MII arrested oocytes, even if they are euploid, will elevate the risk of ensuing embryo aneuploidy following fertilization and completion of the meiosis II division.

Maternal Age Effect following Atrazine Exposure during Development

With our developmental exposure regimen, above (exposed from conception through weaning at 21 dpp), oocyte defects were subsequently observed at 3 months, i.e., long after atrazine was withdrawn (Figures 2–4). Therefore, we explored the relationship between exposure to atrazine during development and the increased chromosome errors seen with advanced maternal age.[6,10,46] The C57BL/6J strain employed here experienced a relatively minor age-related difference in meiotic segregation errors, from a frequency of 1.0% of oocytes (1/105) from 3-month-old animals to 6.9% (2/29) at 15 months of age (Figure 5A). Both low- and high-dose atrazine exposure dramatically exacerbated age-related errors, resulting in chromosomal abnormalities in ≥40% of metaphase-II eggs from 15-month-old animals (8/19 and 9/22 oocytes from low- and high-dose exposure, respectively; Figure 5A). This level is higher than anticipated for additive effects of maternal age plus atrazine exposure (~20%), suggesting that atrazine exposure during development acts synergistically with maternal age, causing very high levels of chromosomally abnormal oocytes in older females.

Sister-chromatid cohesion can only be established during S-phase via the loading of cohesin complexes at replication forks.[48,49] Consequently, progressive depletion of sister-chromatid cohesion in quiescent follicles, leading to chiasma loss (and the appearance of univalent chromosomes) and premature separation of sister chromatids, is a major cause of the high levels of chromosomal

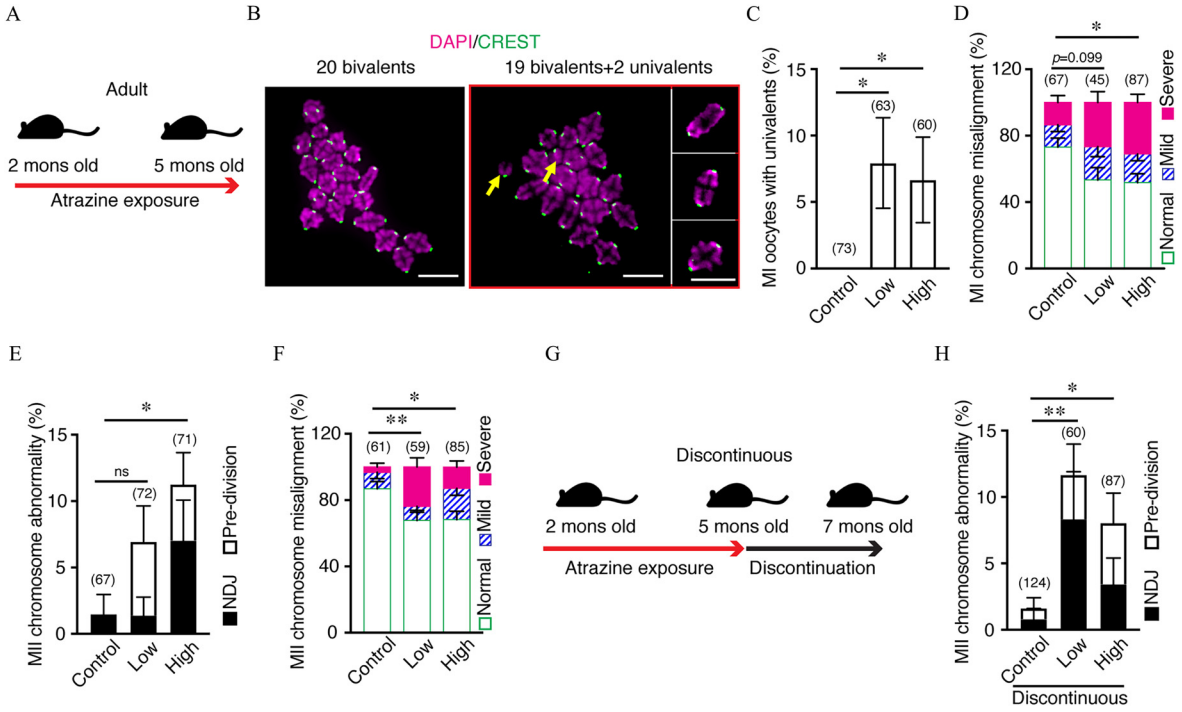

Figure 6. Chromosomal abnormalities and alignment in oocytes following atrazine exposure during adulthood. (A) Schematic of atrazine exposure regimen in adult females. (B) Representative images of MI oocyte chromosome preparations showing a normal nucleus with 20 bivalents and a nucleus containing 19 bivalents and 2 univalents (yellow arrows). Chromosomes shown in insets are from the same cell but were in different fields of view. DNA is colored magenta, and centromeres are green. Scale bars represent 10 μm. (C) Quantification of unconnected univalent chromosomes in chromosome preparations from MI oocytes. Numbers of animals used were 6 (unexposed control), 5 (low dose), and 5 (high dose), respectively (also see Excel Table S19 for summary data). (D) Quantification of chromosome misalignment in metaphase-I oocytes. Numbers of animals used were 4, 3, and 4, respectively (also see Excel Table S20 for summary data). (E) Quantification of chromosomal abnormalities in MII eggs. Numbers of animals used were 7, 6, and 6, respectively (also see Excel Table S21 for summary data). (F) Quantification of chromosome misalignment in metaphase-II eggs. Numbers of animals used were 4, 3, and 4, respectively (also see Excel Table S22 for summary data). (G) Schematic of the discontinuous atrazine exposure regimen. (H) Quantification of chromosomal abnormalities in MII eggs following discontinuous atrazine exposure. Numbers of animals used were 9, 4, and 8, respectively (also see Excel Table S23 for summary data). Numbers of MI oocytes (C,D) and MII eggs (E,F,H) examined are indicated in parentheses above the bars. Error bars represent standard error of a proportion; unidirectional bars are shown in (D–F), and (H) to avoid overlaps. Data were analyzed with Fisher's exact tests. Statistical analysis performed in (D) and (F) compares the distributions of the three alignment classes. MII chromosomal abnormalities were combined for statistical analyses in (E) and (H). Low, 100 μg/L atrazine; High, 33 mg/L. Note: MI, metaphase I; MII, metaphase II; ns, not significant. $^{*}p < 0.05$; $^{**}p < 0.01$.

errors seen in oocytes from older females.[50,51] We assessed whether cohesion is also weakened following atrazine exposure during development. Increased IKD is a readout of weakened cohesion between sister centromeres (Figure 5B).[6,9] Average IKDs were significantly larger in MII nuclei from 15-month-old females following atrazine exposure during development; increasing from 0.94 ± 0.16 μm in unexposed controls to 1.09 ± 0.17 μm and 1.14 ± 0.24 μm in low- and high-dose atrazine groups, respectively (Figure 5C; $p = 0.0195$ and $p = 0.0005$, respectively, one-way ANOVA and Dunnett's tests). Rank distributions of the IKDs of individual sister-chromatid pairs confirmed that centromeric cohesion is weakened following atrazine exposure (Figure 5D; $p < 0.0001$, for both low- and high-dose groups, one-way ANOVA and Dunnett's tests).

Weakening of cohesion following atrazine exposure was further analyzed by quantifying levels of the cohesin complexes that are responsible for sister-chromatid cohesion.[52] MI oocyte chromosomes from 3-month-old females were immunostained for the meiosis-specific cohesin subunit REC8, and fluorescence intensity was calculated (Figure 5E,F; staining was performed at 3 months because REC8 is highly depleted and difficult to detect and quantify in oocytes from very old animals).[6] This analysis revealed lower levels of chromosome-associated cohesin in MI oocytes from atrazine-exposed animals; relative REC8 levels were 9.9% and 7.6% lower in the low- and high-dose atrazine groups, respectively (Figure 5F; $p = 0.0107$ and $p = 0.0608$, respectively, one-way ANOVA and Dunnett's tests; see Excel Table S18 for raw data). Thus, atrazine exposure appears to mimic and thereby exacerbate the effects of maternal aging on oocyte quality by weakening sister-chromatid cohesion.

Atrazine Exposure during Adulthood and Oocyte Abnormalities

Although atrazine exposure during development (gestation through weaning) impacts oocyte divisions, the critical events that occur during fetal development (chromosome synapsis and crossing over) and the early postnatal period (formation of primordial follicles) were only very mildly perturbed (Figure 1). These observations suggest that the most critical exposure window may occur later in life, after primordial follicles have formed. This possibility was tested by exposing adult mice (at 2 months old) to atrazine-contaminated drinking water for 3 months, at the high and low doses detailed above (Figure 6A), after which oocyte divisions were analyzed (Figure 6B–F).

As observed for oocytes from females exposed during development, neither low- nor high-dose atrazine exposure during adulthood affected the maturation efficiency of oocytes when cultured *in vitro*. Specifically, oocytes from all examined groups completed GVBD and PBE with efficiencies of ≥75% (Figure S2D and E; see Excel Tables S28–S31). However, analysis of MI chromosome preparations revealed higher levels of univalent chromosomes in

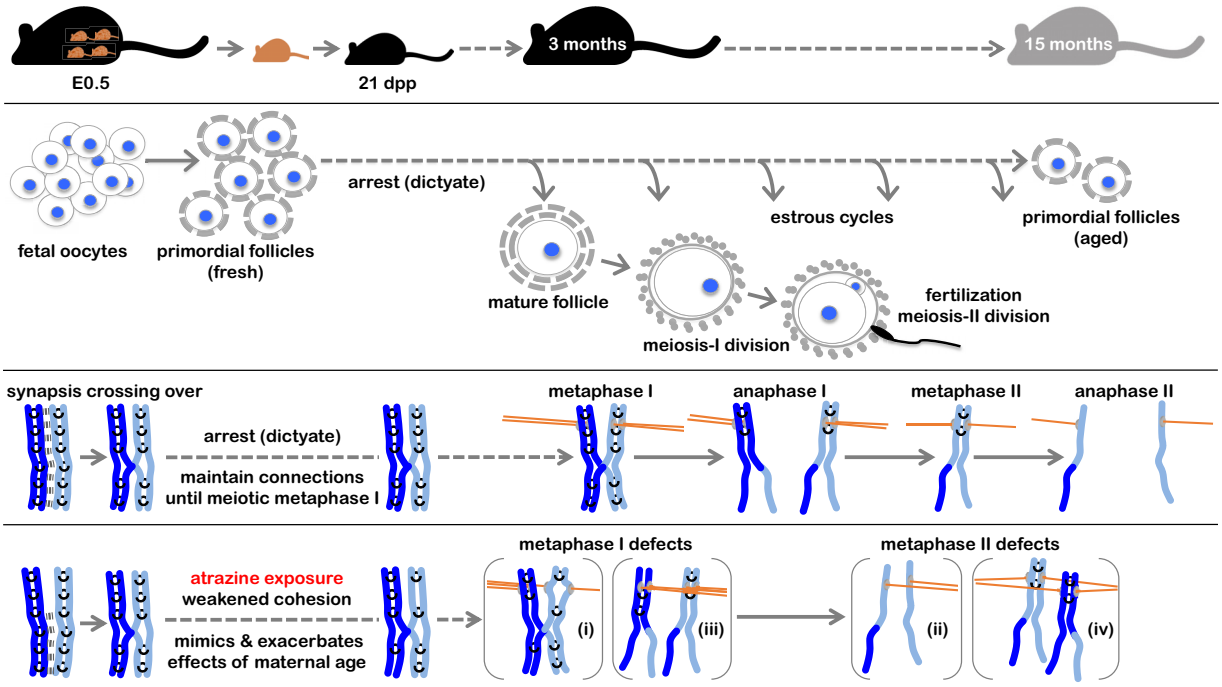

Figure 7. Summary of the long-term effects of atrazine exposure during development on oocyte quality suggested by this study. First row: timeline of mouse development and window of atrazine exposure (developmental exposure regimen) and ages at which parameters of oocyte quality were assessed. Second row: timeline of oocyte development.[59] The events of meiotic prophase-I occur in fetal oocytes, which then arrest around birth and assemble into primordial follicles. With each estrous cycle, cohorts of follicles grow, and meiosis resumes in dominant follicles that are about to be ovulated. The meiosis-I division ensues, and eggs then arrest at MII until fertilization triggers division. Third row: The chromosomal events of meiosis begin in fetal oocytes with chromosome pairing, synapsis (synaptonemal complex indicated by a thick dashed line) and crossing over, shown here for a single pair of homologs (dark and light blue lines).[2] Each homolog comprises a pair of sister chromatids connected by cohesins (black rings); consequently, crossing over results in the connection of homologs, which enables their bipolar alignment on the MI spindle and accurate segregation (disjunction) at meiosis-I (gray disks, kinetochores; orange lines, microtubules). Thus, connections must be maintained in primordial follicles throughout their arrest period. Connections are resolved at anaphase I by the cleavage of cohesins, allowing homologs to separate.[59] Cohesins that connect sister centromeres are protected from cleavage until anaphase II, allowing accurate congression and segregation of sister chromatids.[59] Fourth row: chromosomal errors in oocytes following atrazine exposure. In fetal oocytes, synaptic errors were modestly higher, but numbers of crossovers were not significantly changed. We favor the possibility that primordial follicles are the consequential target of atrazine exposure, which mimics and exacerbates the effects of maternal age by weakening sister-chromatid cohesion, indicated by fewer cohesin complexes (black rings). Weakening of cohesion between centromeres can result in merotelic attachment (i), misalignment at MI, and chromosome lagging at anaphase I.[60] If sister chromatids prematurely separate in anaphase I, the free chromatids are prone to misalign in MII (ii) and missegregate in anaphase II, leading to aneuploidy. Alternatively, sister chromatids may prematurely separate in MII and missegregate in anaphase II. Loss of cohesion distal to crossover points results in prematurely separated univalents (iii), which can co-orient at MI and cosegregate at anaphase I (NDJ), resulting in aneuploidy in MII (iv) and in the ovum pronucleus following fertilization. Alternatively, the sister chromatids of a univalent may undergo premature segregation in anaphase I (reverse segregation[50,61]). Note: MI, metaphase I; MII, metaphase II; NDJ, nondisjunction.

oocytes from atrazine-exposed animals (Figure 6B,C). Univalents were never observed in controls but were present in 7.9% (5/63) and 6.7% (4/60) of oocytes from the low- and high-dose atrazine groups, respectively ($p = 0.0195$ and $p = 0.0391$ respectively, Fisher's exact test). Univalent formation is consistent with a weakening of sister-chromatid cohesion following atrazine exposure (Figure 5E,F).

The presence of univalents during MI anticipates defective congression and segregation.[4] Indeed, nearly 50% of oocytes (21/45 and 42/87) from both low- and high-dose atrazine-exposed adults had congression defects at MI (Figure 6D). Comparison of the three alignment classes showed significantly higher levels of misalignment for the high-dose group ($p = 0.0170$, Fisher's exact test), but not for the low-dose group ($p = 0.0991$). However, when analyzed as a simple proportion, oocytes with chromosome misalignment (mild + severe) were significantly higher in the low-dose group ($p = 0.0429$). In the high-dose group, severe chromosome misalignment (≥3 chromosomes) was seen in 31.0% of cells (27/87) in comparison with 13.4% of control oocytes (9/67). These levels are much higher than expected if univalents were the sole cause of misalignment, implying that atrazine may cause additional defects that perturb congression, such as merotelic spindle attachment, which can result from weakening of cohesion between the centromeres of sister chromatids (Figure 5B–D)[51,53] or spindle abnormalities, as described for other endocrine disruptors such as bisphenol A.[54,55]

In MII-arrested oocytes, chromosomal abnormalities were observed in 6.9% (5/72) and 11.3% (8/71) of oocytes from the low- and high-dose groups, respectively, in comparison with only 1.5% (1/67) in controls (Figure 6E; again, only the high-dose group was significantly different from controls, $p = 0.0337$, Fisher's exact test). Chromosome congression was also analyzed in MII-arrested eggs, revealing misalignment in >30% of eggs from atrazine-exposed groups (19/59 and 27/85 in low- and high-dose groups, respectively) in comparison with 13.1% (8/61) in controls (Figure 6F; $p = 0.0033$ and $p = 0.0302$ for low- and high-dose groups, respectively, Fisher's exact test).

Atrazine Exposure in Adults and Long-Term Impacts on Oocyte Quality

To test whether exposure in adulthood has long-term effects, as seen following developmental exposure, mice were given

atrazine-contaminated drinking water between 2 and 5 months of age, followed by pure water for an additional 2 months before MII-arrested oocytes were analyzed (Figure 6G). This analysis confirmed that the effects of atrazine exposure were persistent, with significantly higher levels of chromosomal abnormalities being observed in both low- and high-dose groups, and were of the same magnitude as those seen following continuous exposure immediately prior to oocyte analysis (Figure 6H; compare with Figure 6E).

Discussion

In this study, chronic ingestion of low levels of atrazine via drinking water was associated with persistent negative effects on oocyte quality in mice, with defects being detected during meiosis, fertilization, and early development. To the best of our knowledge, we have provided the first clear evidence that atrazine exposure can perturb oocyte chromosome segregation during both meiotic divisions and can exacerbate the effects of maternal age on oocyte quality. Atrazine exposure during adulthood was associated with defects in oocyte divisions that were the same magnitude as those seen following developmental exposure. Although it is formally possible that exposure during development and adulthood cause the same defects through distinct mechanisms, the most straightforward interpretation is that the critical period for atrazine exposure occurs after the perinatal period when ovarian reserves are established. These considerations suggest that established primordial follicles may be a primary target of atrazine perturbation. Alternatively, or in addition, atrazine exposure may alter oocyte growth, which has also been associated with defects in chromosome congression and segregation.[56] Mechanistically, one cause of atrazine's effects appears to be weakening of sister-chromatid cohesion, effectively mimicking a well-characterized aspect of oocyte aging.[8,52] This mechanism is summarized and synthesized into a model that reconciles the chromosomal perturbations we observed following atrazine exposure (Figure 7).

Meiotic Prophase I and Follicle Formation

Defects in homolog synapsis were higher following exposure *in utero* (Figure 1C), but the impact on crossing over and oocyte survival was negligible (Figure 1E–G). A previous mouse study detected slightly higher crossover levels ($\sim$6% fewer MLH1 foci) following acute dosing of pregnant dams (100 mg/kg/d), perhaps as a consequence of the higher atrazine dose employed (12- and 4,000-fold higher than the two doses employed in our study).[28] Slightly higher numbers of multi-oocyte follicles were detected following exposure to $\sim$8.25 mg/kg/d atrazine (this study, Figure 1H,I) and to the much higher dose of 100 mg/kg/d.[28] This defect could be explained by documented increases in progesterone in rats following atrazine exposure at 100 mg/kg/d[30] or higher,[19] because Chen et al. (2007) showed that high levels of progesterone impeded oocyte-nest breakdown and the assembly of primordial follicles in mouse ovaries.[57] Moreover, the higher levels of ovulation that we observed following atrazine exposure (Figure 2A) could also be explained by elevated progesterone, because in an *ex vivo* ovary culture model, 100 ng/mL progesterone was able to promote initial follicle growth and increase the numbers of ovulated oocytes (although a higher concentration, 1 µg/mL, inhibited ovulation).[58]

Weakened Cohesion and Chromosomal Abnormalities following Atrazine Exposure

Atrazine exposure was associated with negative consequences for oocyte meiosis specifically: *a*) chromosome misalignment at both MI and MII, and *b*) chromosome missegregation and predivision presenting in MII. Because exposure during development or adulthood was associated with similar levels of chromosome errors, we favor the idea that quiescent oocytes present in primordial follicles are the consequential targets of atrazine (Figure 7, second row). Efficient chromosome segregation requires that primordial follicles maintain a critical level of sister-chromatid cohesion until they mature and complete meiotic divisions.[59] Optimal cohesion has two critical functions for chromosome alignment and segregation during the two divisions of meiosis:

1. Cohesion between centromeres helps organize the kinetochores of sister chromatids into a fused structure required for monopolar attachment and thus correct orientation on the MI spindle (Figure 7, third row).[59,60] Suboptimal centromere cohesion causes premature individualization of kinetochores, allowing bipolar attachment of sister chromatids to the MI spindle (merotelic attachment) abnormality [(i) in Figure 7, fourth row]. Premature segregation of sister chromatids may then ensue at anaphase I, with a high probability of producing an aneuploid ovum pronucleus after anaphase II. Even without erroneous segregation of sister chromatids at anaphase I, weakening of centromere cohesion may lead to premature separation and co-orientation of sister chromatids in MII [abnormality (ii) in Figure 7, fourth row], also a high risk for aneuploidy.
2. Cohesion between chromosome arms maintains connections (chiasmata) between homolog pairs that enable their stable bipolar orientation and congression on the MI spindle (Figure 7, third row). Suboptimal arm cohesion can lead to premature loss of interhomolog connections, i.e. univalent formation. Univalents may co-orientate on the MI spindle [abnormality (iii) Figure 7, fourth row] and cosegregate (nondisjunction) at anaphase I. The resulting aneuploidy at MII [abnormality (iv) Figure 7, fourth row], will result in disomy in the ovum pronucleus. Alternatively, the sister chromatids of a univalent may biorient in MI and segregate in anaphase I ("reverse segregation").[50,61]

Thus, the weakening of sister-chromatid cohesion associated with atrazine exposure can explain the higher levels of chromosome misalignment and abnormalities seen in both MI and MII oocytes. However, the observed cohesion loss may not necessarily be a direct consequence of atrazine exposure; instead, it may be a new facet of a broader effect of endocrine-disrupting chemicals on oocyte meiotic divisions.[54,55] Moreover, weakened cohesion seems unlikely to be the sole mechanism of the meiotic errors observed following atrazine exposure. Notably, changes in oocyte growth following endocrine perturbation have been associated with increased frequencies of chromosome defects.[62]

Maternal Age Effect

Weakened sister-chromatid cohesion can also help explain how atrazine exposure exacerbated the effects of maternal age on oocyte quality. Egg aneuploidy increases with advancing maternal age.[8,52] Specifically, a physiological aging process associated with ovulation is inferred to cause progressive loss of cohesion in primordial follicles.[63] When residual cohesion falls below a critical threshold (estimated at $\sim$10% of starting levels in mice),[6,8] chromosomal errors increase dramatically. Thus, atrazine exposure appeared to mimic one important facet of maternal aging, suggesting that the critical threshold of cohesion required for accurate segregation was reached at a younger age and in a larger fraction of oocytes—hence the high levels of chromosomal errors seen in eggs from 15-month-old animals.

Fertilization and Blastocyst Integrity following Atrazine Exposure

Apoptotic cells were generally increased in blastocysts derived from eggs of atrazine-exposed animals, and their numbers were very variable (1.7% to 22.2% of total cells; see Excel Table S10). Blastocysts with a high fraction of apoptotic cells could be a consequence of problems present in the zygote or very early embryo, such as aneuploidy, which does not necessarily impede blastocyst formation but leads to increased apoptosis.[64–66] The reason for the lower fertilization efficiency of eggs following atrazine exposure is less clear. Possibly, atrazine causes epigenetic changes that perturb the transcriptional responses required for optimal maturation and fertilization.[28] Together, our analysis reveals that atrazine exposure during development is associated with negative impacts on various indicators of oocyte quality including higher levels of fragmented MII eggs, lower fertilization rates, and higher levels of apoptosis in blastocysts.

Mechanism of Action

How atrazine exposure caused the meiotic aberrations and cohesion weakening observed here remains unclear. Across vertebrate classes, atrazine acts through multiple mechanisms to disrupt the neuroendocrine system,[67] especially steroidogenesis pathways.[11,19,30] Atrazine may also impact oocyte function through documented increases in oxidative stress, including mitochondrial dysfunction seen in both aquatic organisms[68] and mammals.[28,68] Moreover, fetal exposure to high levels of atrazine caused lower expression of genes involved in protection from oxidative stress in the ovaries of 6-d-old mice.[28] It will be important to establish whether similar effects on the oxidative stress response are caused by low-dose atrazine exposure at different times during development and in adults. Importantly, oxidative damage is suggested to be a possible cause of cohesion loss as primordial oocytes age[68–70] and is therefore a candidate mechanism to explain how atrazine exposure interacts with maternal age to reduce oocyte quality. Also, given that ovulation frequency appears to be the physiological basis of oocyte aging,[63] the higher levels of ovulation observed following atrazine exposure could accelerate this process.

Extensive similarities between mouse and human oocytes suggest that our findings may be pertinent for the reproductive health of human females and set the stage for expanded studies in rodents, nonhuman primates, and humans that will inform and guide the public, health workers, and policymakers.

Acknowledgments

The authors thank R. Schultz and members of the Hunter Lab for support and discussions; and S. Keeney for the kind gift of REC8 antibodies.

Y.Y. and N.H. designed the research; Y.Y., C.S., R.M., and M.H. performed the experiments; Y.Y., S.L., C.S., R.M., C.K, T.W., and N.H. analyzed data; Y.Y. and N.H. wrote the paper.

This research was supported by the National Institute of Environmental Health Sciences under Award P30ES023513. N.H. is an investigator at the Howard Hughes Medical Institute, which also supported this study.

References

1. Canipari R, De Santis L, Cecconi S. 2020. Female fertility and environmental pollution. Int J Environ Res Public Health 17(23):8802, https://doi.org/10.3390/ijerph17238802.
2. Hunter N. 2015. Meiotic recombination: the essence of heredity. Cold Spring Harb Perspect Biol 7(12):a016618, https://doi.org/10.1101/cshperspect.a016618.
3. Jones KT. 2008. Meiosis in oocytes: predisposition to aneuploidy and its increased incidence with age. Hum Reprod Update 14(2):143–158, PMID: 18084010, https://doi.org/10.1093/humupd/dmm043.
4. Nagaoka SI, Hodges CA, Albertini DF, Hunt PA. 2011. Oocyte-Specific differences in Cell-Cycle control create an innate susceptibility to meiotic errors. Curr Biol 21(8):651–657. PMID: 21497085, https://doi.org/10.1016/j.cub.2011.03.003.
5. Gruhn JR, Zielinska AP, Shukla V, Blanshard R, Capalbo A, Cimadomo D, et al. 2019. Chromosome errors in human eggs shape natural fertility over reproductive life span. Science 365(6460):1466–1469, PMID: 31604276, https://doi.org/10.1126/science.aav7321.
6. Chiang T, Duncan FE, Schindler K, Schultz RM, Lampson MA. 2010. Evidence that weakened centromere cohesion is a leading cause of Age-Related aneuploidy in oocytes. Curr Biol 20(17):1522–1528, PMID: 20817534, https://doi.org/10.1016/j.cub.2010.06.069.
7. Duncan FE, Hornick JE, Lampson MA, Schultz RM, Shea LD, Woodruff TK. 2012. Chromosome cohesion decreases in human eggs with advanced maternal age. Aging Cell 11(6):1121–1124, PMID: 22823533, https://doi.org/10.1111/j.1474-9726.2012.00866.x.
8. Jessberger R. 2012. Age-related aneuploidy through cohesion exhaustion. EMBO Rep 13(6):539–546, PMID: 22565322, https://doi.org/10.1038/embor.2012.54.
9. Lagirand-Cantaloube J, Ciabrini C, Charrasse S, Ferrieres A, Castro A, Anahory T, et al. 2017. Loss of centromere cohesion in aneuploid human oocytes correlates with decreased kinetochore localization of the sac proteins Bub1 and Bubr1. Sci Rep 7:44001, PMID: 28287092, https://doi.org/10.1038/srep44001.
10. Lister LM, Kouznetsova A, Hyslop LA, Kalleas D, Pace SL, Barel JC, et al. 2010. Age-Related meiotic segregation errors in mammalian oocytes are preceded by depletion of cohesin and Sgo2. Curr Biol 20(17):1511–1521, PMID: 20817533, https://doi.org/10.1016/j.cub.2010.08.023.
11. Hayes TB, Anderson LL, Beasley VR, de Solla SR, Iguchi T, Ingraham H, et al. 2011. Demasculinization and feminization of male gonads by atrazine: consistent effects across vertebrate classes. J Steroid Biochem Mol Biol 127(1–2):64–73, PMID: 21419222, https://doi.org/10.1016/j.jsbmb.2011.03.015.
12. Udiković-Kolić N, Scott C, Martin-Laurent F. 2012. Evolution of atrazine-degrading capabilities in the environment. Appl Microbiol Biotechnol 96(5):1175–1189, PMID: 23076592, https://doi.org/10.1007/s00253-012-4495-0.
13. He H, Liu Y, You S, Liu J, Xiao H, Tu Z. 2019. A review on recent treatment technology for herbicide atrazine in contaminated environment. Int J Environ Res Public Health 16(24):5129, https://doi.org/10.3390/ijerph16245129.
14. National Primary Drinking Water Regulations. U.S. Environmental Protection Agency. https://www.epa.gov/sites/default/files/2016-06/documents/npwdr_complete_table.pdf [accessed 10 October 2022].
15. World Health Organization. 2011. *Guidelines for Drinking-Water Quality*. 4th ed. Geneva, Switzerland: World Health Organization.
16. Hatfield JL, Wesley CK, Prueger JH, Pfeiffer RL. 1996. Herbicide and nitrate distribution in Central Iowa rainfall. J Environ Qual 25(2):259–264, https://doi.org/10.2134/jeq1996.00472425002500020008x.
17. Murphy MB, Hecker M, Coady KK, Tompsett AR, Jones PD, Du Preez LH, et al. 2006. Atrazine concentrations, gonadal gross morphology and histology in ranid frogs collected in Michigan agricultural areas. Aquat Toxicol 76(3–4):230–245, PMID: 16300839, https://doi.org/10.1016/j.aquatox.2005.09.010.
18. Alavanja MCR, Hoppin JA, Kamel F. 2004. Health effects of chronic pesticide exposure: cancer and neurotoxicity. Annu Rev Public Health 25(1):155–197, PMID: 15015917, https://doi.org/10.1146/annurev.publhealth.25.101802.123020.
19. Wirbisky S, Freeman J. 2015. Atrazine exposure and reproductive dysfunction through the hypothalamus-pituitary-gonadal (HPG) axis. Toxics 3(4):414–450, PMID: 28713818, https://doi.org/10.3390/toxics3040414.
20. Hayes TB, Collins A, Lee M, Mendoza M, Noriega N, Stuart AA, et al. 2002. Hermaphroditic, demasculinized frogs after exposure to the herbicide atrazine at low ecologically relevant doses. Proc Natl Acad Sci USA 99(8):5476–5480, PMID: 11960004, https://doi.org/10.1073/pnas.082121499.
21. Rohr JR, McCoy KA. 2010. A qualitative meta-analysis reveals consistent effects of atrazine on freshwater fish and amphibians. Environ Health Perspect 118(1):20–32, PMID: 20056568, https://doi.org/10.1289/ehp.0901164.
22. Stanko JP, Enoch RR, Rayner JL, Davis CC, Wolf DC, Malarkey DE, et al. 2010. Effects of prenatal exposure to a low dose atrazine metabolite mixture on pubertal timing and prostate development of male Long-Evans rats. Reprod Toxicol 30(4):540–549, PMID: 20727709, https://doi.org/10.1016/j.reprotox.2010.07.006.
23. Rosenberg BG, Chen H, Folmer J, Liu J, Papadopoulos V, Zirkin BR. 2008. Gestational exposure to atrazine: effects on the postnatal development of male offspring. J Androl 29(3):304–311, PMID: 17978342, https://doi.org/10.2164/jandrol.107.003020.
24. Abarikwu SO, Adesiyan AC, Oyeloja TO, Oyeyemi MO, Farombi EO. 2010. Changes in sperm characteristics and induction of oxidative stress in the testis and epididymis of experimental rats by a herbicide, atrazine. Arch Environ Contam Toxicol 58(3):874–882, PMID: 19672647, https://doi.org/10.1007/s00244-009-9371-2.

25. Song Y, Jia ZC, Chen JY, Hu JX, Zhang LS. 2014. Toxic effects of atrazine on reproductive system of male rats. Biomed Environ Sci 27(4):281–288, PMID: 24758756, https://doi.org/10.3967/bes2014.050.
26. Gely-Pernot A, Hao C, Becker E, Stuparevic I, Kervarrec C, Chalmel F, et al. 2015. The epigenetic processes of meiosis in male mice are broadly affected by the widely used herbicide atrazine. BMC Genomics 16(1):885, PMID: 26518232, https://doi.org/10.1186/s12864-015-2095-y.
27. Swan SH, Kruse RL, Liu F, Barr DB, Drobnis EZ, Redmon JB, et al. 2003. Semen quality in relation to biomarkers of pesticide exposure. Environ Health Perspect 111(12):1478–1484, PMID: 12948887, https://doi.org/10.1289/ehp.6417.
28. Gely-Pernot A, Saci S, Kernanec P-Y, Hao C, Giton F, Kervarrec C, et al. 2017. Embryonic exposure to the widely-used herbicide atrazine disrupts meiosis and normal follicle formation in female mice. Sci Rep 7(1):3526, PMID: 28615648, https://doi.org/10.1038/s41598-017-03738-1.
29. Davis LK, Murr AS, Best DS, Fraites MJP, Zorrilla LM, Narotsky MG, et al. 2011. The effects of prenatal exposure to atrazine on pubertal and postnatal reproductive indices in the female rat. Reprod Toxicol 32(1):43–51, PMID: 21530638, https://doi.org/10.1016/j.reprotox.2011.04.004.
30. Goldman JM, Davis LK, Murr AS, Cooper RL. 2013. Atrazine-induced elevation or attenuation of the LH surge in the ovariectomized, estrogen-primed female rat: role of adrenal progesterone. Reproduction 146(4):305–314, PMID: 23847262, https://doi.org/10.1530/REP-13-0011.
31. Shibayama H, Kotera T, Shinoda Y, Hanada T, Kajihara T, Ueda M, et al. 2009. Collaborative work on evaluation of ovarian toxicity. 14) Two- or four-week repeated-dose studies and fertility study of atrazine in female rats. J Toxicol Sci 34 Suppl 1:SP147–155, PMID: 19265281, https://doi.org/10.2131/jts.34.s147.
32. Taketa Y, Yoshida M, Inoue K, Takahashi M, Sakamoto Y, Watanabe G, et al. 2011. Differential stimulation pathways of progesterone secretion from newly formed corpora lutea in rats treated with ethylene glycol monomethyl ether, sulpiride, or atrazine. Toxicol Sci 121(2):267–278, PMID: 21427058, https://doi.org/10.1093/toxsci/kfr062.
33. Rayner JL, Enoch RR, Fenton SE. 2005. Adverse effects of prenatal exposure to atrazine during a critical period of mammary gland growth. Toxicol Sci 87(1):255–266, PMID: 15933227, https://doi.org/10.1093/toxsci/kfi213.
34. Gojmerac T, Kartal B, Curić S, Zurić M, Kusević S, Cvetnić Z. 1996. Serum biochemical changes associated with cystic ovarian degeneration in pigs after atrazine treatment. Toxicol Lett 85(1):9–15, PMID: 8619262, https://doi.org/10.1016/0378-4274(96)03631-4.
35. Chevrier C, Limon G, Monfort C, Rouget F, Garlantézec R, Petit C, et al. 2011. Urinary biomarkers of prenatal atrazine exposure and adverse birth outcomes in the PELAGIE birth cohort. Environ Health Perspect 119(7):1034–1041, PMID: 21367690, https://doi.org/10.1289/ehp.1002775.
36. Munger R, Isacson P, Hu S, Burns T, Hanson J, Lynch CF, et al. 1997. Intrauterine growth retardation in Iowa communities with herbicide-contaminated drinking water supplies. Environ Health Perspect 105(3):308–314, PMID: 9171992, https://doi.org/10.1289/ehp.97105308.
37. Stayner LT, Almberg K, Jones R, Graber J, Pedersen M, Turyk M. 2017. Atrazine and nitrate in drinking water and the risk of preterm delivery and low birth weight in four Midwestern states. Environ Res 152:294–303, PMID: 27816866, https://doi.org/10.1016/j.envres.2016.10.022.
38. Villanueva CM, Durand G, Coutté MB, Chevrier C, Cordier S. 2005. Atrazine in municipal drinking water and risk of low birth weight, preterm delivery, and small-for-gestational-age status. Occup Environ Med 62(6):400–405, PMID: 15901888, https://doi.org/10.1136/oem.2004.016469.
39. Yalkowsky SH, He Y, Jain P. 2019. Handbook of Aqueous Solubility Data. Boca Raton, FL: CRC Press.
40. Yun Y, Ito M, Sandhu S, Hunter N. 2021. Cytological monitoring of meiotic crossovers in spermatocytes and oocytes. Methods Mol Biol 2153:267–286, PMID: 32840786, https://doi.org/10.1007/978-1-0716-0644-5_19.
41. Maier NK, Ma J, Lampson MA, Cheeseman IM. 2021. Separase cleaves the kinetochore protein Meikin at the meiosis I/II transition. Dev Cell 56(15):2192–2206.e8, PMID: 34331869, https://doi.org/10.1016/j.devcel.2021.06.019.
42. Mihajlović AI, Haverfield J, FitzHarris G. 2021. Distinct classes of lagging chromosome underpin age-related oocyte aneuploidy in mouse. Dev Cell 56(16):2273–2283.e3, PMID: 34428397, https://doi.org/10.1016/j.devcel.2021.07.022.
43. Hunter N. 2017. Oocyte quality control: causes, mechanisms, and consequences. Cold Spring Harb Symp Quant Biol 82:235–247, PMID: 29743337, https://doi.org/10.1101/sqb.2017.82.035394.
44. Pepling ME. 2012. Follicular assembly: mechanisms of action. Reproduction 143(2):139–149, PMID: 22065859, https://doi.org/10.1530/REP-11-0299.
45. Lane SIR, Yun Y, Jones KT. 2012. Timing of anaphase-promoting complex activation in mouse oocytes is predicted by microtubule-kinetochore attachment but not by bivalent alignment or tension. Development 139(11):1947–1955, PMID: 22513370, https://doi.org/10.1242/dev.077040.
46. Yun Y, Lane SIR, Jones KT. 2014. Premature dyad separation in meiosis II is the major segregation error with maternal age in mouse oocytes. Development 141(1):199–208, PMID: 24346700, https://doi.org/10.1242/dev.100206.
47. Yun Y, Holt JE, Lane S, McLaughlin E, Merriman J, Jones K. 2014. Reduced ability to recover from spindle disruption and loss of kinetochore spindle assembly checkpoint proteins in oocytes from aged mice. Cell Cycle 13(12):1938–1947, PMID: 24758999, https://doi.org/10.4161/cc.28897.
48. Zuilkoski CM, Skibbens RV. 2022. Integrating sister chromatid cohesion establishment to DNA replication. Genes (Basel) 13(4):625. PMID: 35456431, https://doi.org/10.3390/genes13040625.
49. Murayama Y, Samora CP, Kurokawa Y, Iwasaki H, Uhlmann F. 2018. Establishment of DNA-DNA interactions by the cohesin ring. Cell 172(3):465–477.e15, PMID: 29358048, https://doi.org/10.1016/j.cell.2017.12.021.
50. Sakakibara Y, Hashimoto S, Nakaoka Y, Kouznetsova A, Höög C, Kitajima TS. 2015. Bivalent separation into univalents precedes age-related meiosis I errors in oocytes. Nat Commun 6:7550, PMID: 26130582, https://doi.org/10.1038/ncomms8550.
51. Zielinska AP, Holubcova Z, Blayney M, Elder K, Schuh M. 2015. Sister kinetochore splitting and precocious disintegration of bivalents could explain the maternal age effect. elife 4:e11389, PMID: 26670547, https://doi.org/10.7554/eLife.11389.
52. Cheng JM, Liu YX. 2017. Age-Related loss of cohesion: causes and effects. Int J Mol Sci 18(7):1578, https://doi.org/10.3390/ijms18071578.
53. Shomper M, Lappa C, FitzHarris G. 2014. Kinetochore microtubule establishment is defective in oocytes from aged mice. Cell Cycle 13(7):1171–1179, PMID: 24553117, https://doi.org/10.4161/cc.28046.
54. Hunt PA, Koehler KE, Susiarjo M, Hodges CA, Ilagan A, Voigt RC, et al. 2003. Bisphenol A exposure causes meiotic aneuploidy in the female mouse. Curr Biol 13(7):546–553, https://doi.org/10.1016/S0960-9822(03)00189-1.
55. Muhlhauser A, Susiarjo M, Rubio C, Griswold J, Gorence G, Hassold T, et al. 2009. Bisphenol A effects on the growing mouse oocyte are influenced by diet. Biol Reprod 80(5):1066–1071, PMID: 19164168, https://doi.org/10.1095/biolreprod.108.074815.
56. Hodges CA, Ilagan A, Jennings D, Keri R, Nilson J, Hunt PA. 2002. Experimental evidence that changes in oocyte growth influence meiotic chromosome segregation. Hum Reprod 17(5):1171–1180, PMID: 11980735, https://doi.org/10.1093/humrep/17.5.1171.
57. Chen Y, Jefferson WN, Newbold RR, Padilla-Banks E, Pepling ME. 2007. Estradiol, progesterone, and genistein inhibit oocyte nest breakdown and primordial follicle assembly in the neonatal mouse ovary in vitro and in vivo. Endocrinology 148(8):3580–3590, PMID: 17446182, https://doi.org/10.1210/en.2007-0088.
58. Komatsu K, Masubuchi S. 2017. The concentration-dependent effect of progesterone on follicle growth in the mouse ovary. J Reprod Dev 63(3):271–277, PMID: 28321005, https://doi.org/10.1262/jrd.2016-154.
59. Greaney J, Wei Z, Homer H. 2018. Regulation of chromosome segregation in oocytes and the cellular basis for female meiotic errors. Hum Reprod Update 24(2):135–161, PMID: 29244163, https://doi.org/10.1093/humupd/dmx035.
60. Wang LI, Das A, McKim KS. 2019. Sister centromere fusion during meiosis I depends on maintaining cohesins and destabilizing microtubule attachments. PLoS Genet 15(5):e1008072, PMID: 31150390, https://doi.org/10.1371/journal.pgen.1008072.
61. Ottolini CS, Newnham L, Capalbo A, Natesan SA, Joshi HA, Cimadomo D, et al. 2015. Genome-wide maps of recombination and chromosome segregation in human oocytes and embryos show selection for maternal recombination rates. Nat Genet 47(7):727–735, PMID: 25985139, https://doi.org/10.1038/ng.3306.
62. Machtinger R, Orvieto R. 2014. Bisphenol A, oocyte maturation, implantation, and IVF outcome: review of animal and human data. Reprod Biomed Online 29(4):404–410, PMID: 25154017, https://doi.org/10.1016/j.rbmo.2014.06.013.
63. Chatzidaki EE, Powell S, Dequeker BJH, Gassler J, Silva MCC, Tachibana K. 2021. Ovulation suppression protects against chromosomal abnormalities in mouse eggs at advanced maternal age. Curr Biol 31(18):4038–4051.e7, PMID: 34314679, https://doi.org/10.1016/j.cub.2021.06.076.
64. Bolton H, Graham SJL, Van der Aa N, Kumar P, Theunis K, Fernandez Gallardo E, et al. 2016. Mouse model of chromosome mosaicism reveals lineage-specific depletion of aneuploid cells and normal developmental potential. Nat Commun 7:11165, PMID: 27021558, https://doi.org/10.1038/ncomms11165.
65. Rubio C, Rodrigo L, Mercader A, Mateu E, Buendía P, Pehlivan T, et al. 2007. Impact of chromosomal abnormalities on preimplantation embryo development. Prenat Diagn 27(8):748–756, PMID: 17546708, https://doi.org/10.1002/pd.1773.

66. Tsuiko O, Jatsenko T, Parameswaran Grace LK, Kurg A, Vermeesch JR, Lanner F, et al. 2019. A speculative outlook on embryonic aneuploidy: can molecular pathways be involved? Dev Biol 447(1):3–13, PMID: 29391166, https://doi.org/10.1016/j.ydbio.2018.01.014.
67. Graceli JB, Dettogni RS, Merlo E, Niño O, da Costa CS, Zanol JF, et al. 2020. The impact of endocrine-disrupting chemical exposure in the mammalian hypothalamic-pituitary axis. Mol Cell Endocrinol 518:110997, PMID: 32841708, https://doi.org/10.1016/j.mce.2020.110997.
68. Semren TŽ, Žunec S, Pizent A. 2018. Oxidative stress in triazine pesticide toxicity: a review of the main biomarker findings. Arh Hig Rada Toksikol 69(2):109–125, PMID: 29990300, https://doi.org/10.2478/aiht-2018-69-3118.
69. Perkins AT, Das TM, Panzera LC, Bickel SE. 2016. Oxidative stress in oocytes during midprophase induces premature loss of cohesion and chromosome segregation errors. Proc Natl Acad Sci USA 113(44):E6823–E6830, PMID: 27791141, https://doi.org/10.1073/pnas.1612047113.
70. Sasaki H, Hamatani T, Kamijo S, Iwai M, Kobanawa M, Ogawa S, et al. 2019. Impact of oxidative stress on age-associated decline in oocyte developmental competence. Front Endocrinol (Lausanne) 10:811, PMID: 31824426, https://doi.org/10.3389/fendo.2019.00811.